

Astrophysics of Extreme Mass Ratio Inspirals

Matteo Bonetti - University of Milano-Bicocca

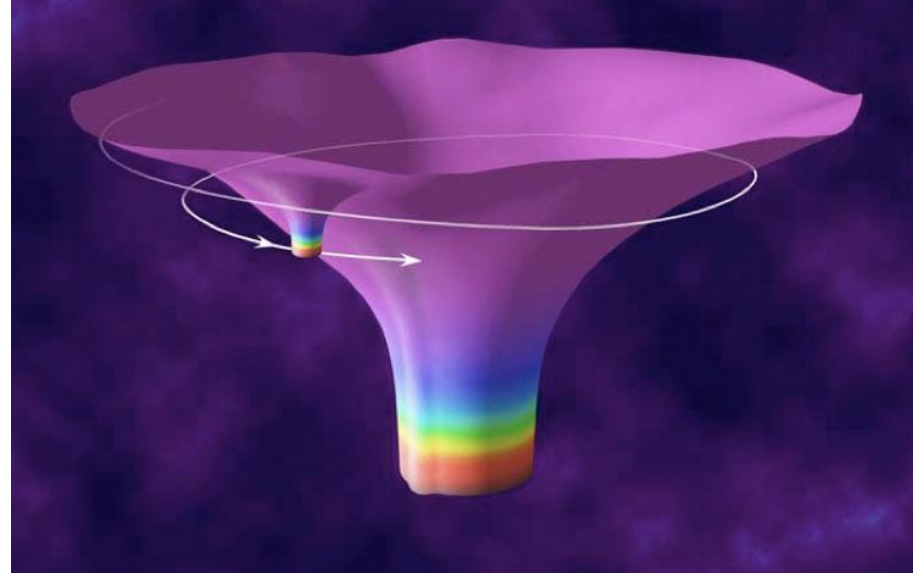
What are EMRIs?

EMRIs features:

Binary systems with mass ratio between 10^{-9} and 10^{-4}

Astrophysically relevant systems involve a massive black hole hosted in the centre of a galaxy.

We generally think them as formed by compact objects (even though not always the case).

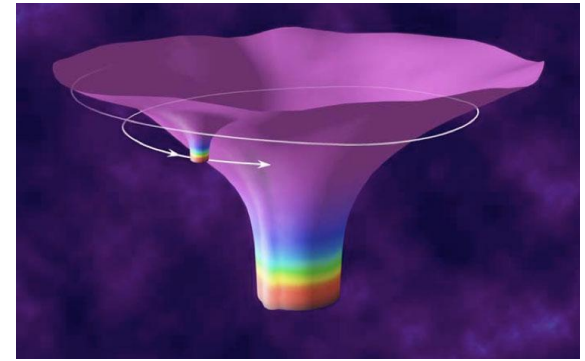


What are EMRIs?

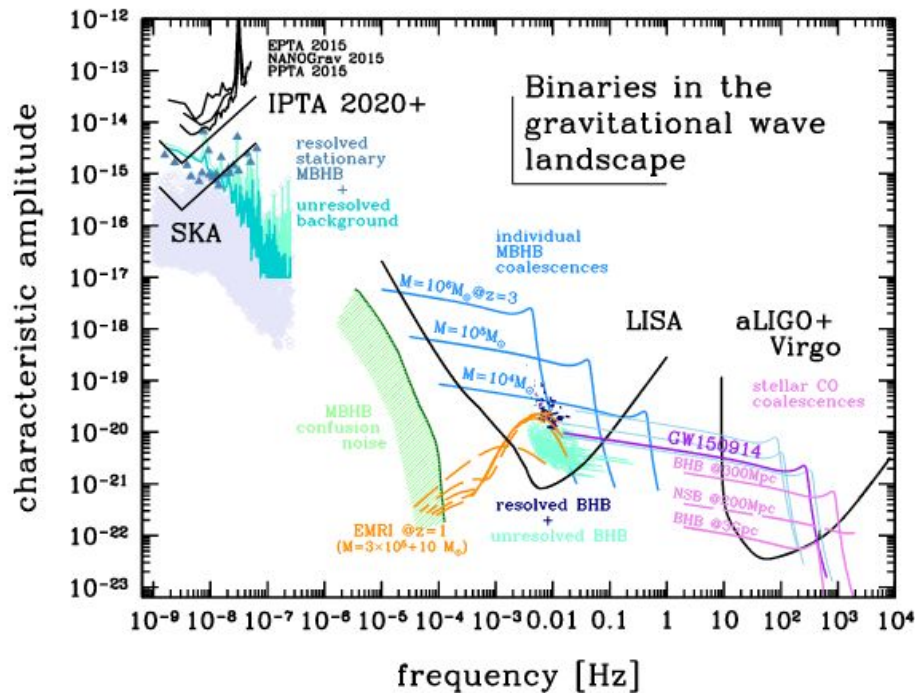
Possible kind of objects as EMRI secondary:

- Stellar mass black hole (most standard case)
- Neutron star
- White dwarf (can be disrupted)
- Stars (can be disrupted)
- Others?

The kind of object involved might be connected to the formation mechanism (?)



What are EMRIs?



EMRIs will be primary GW sources for LISA science case

$$f_{GW,max} = 4 \times 10^{-3} \left(\frac{M}{10^6 M_\odot} \right)^{-1} \text{ Hz}$$

$$h = \sqrt{\frac{32}{5} \frac{(G M_c)^{5/3}}{c^4 d_L} (\pi f_{GW})^{2/3}}$$

Why EMRIs are important?

Orbital parameters
of the binary

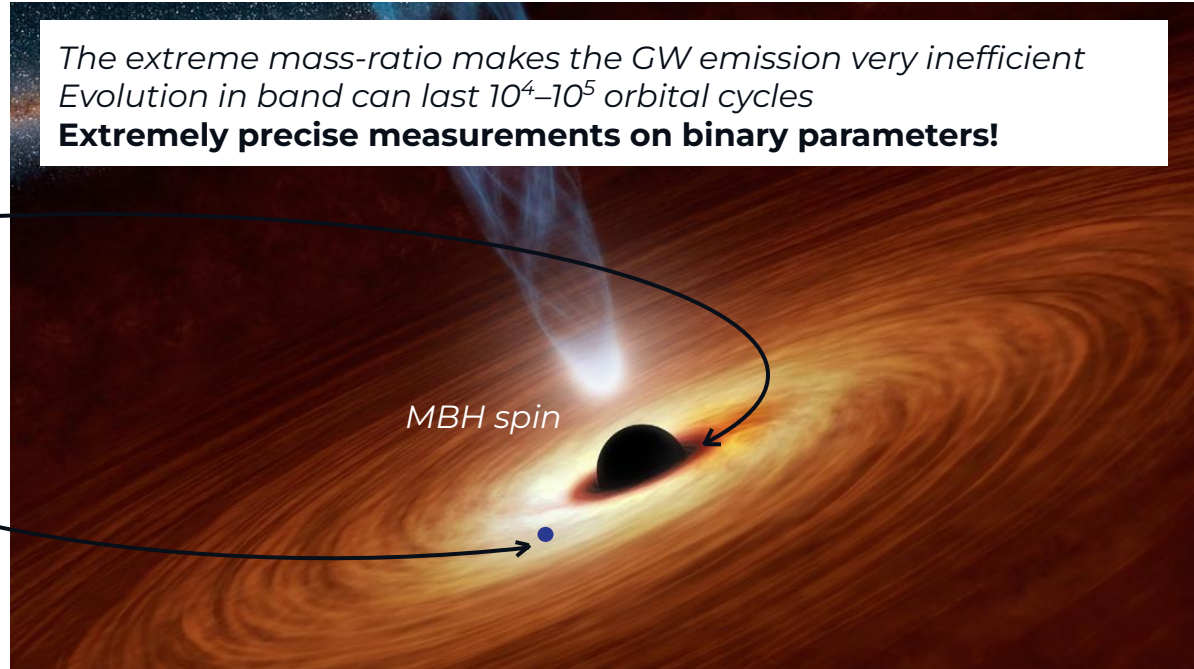
Redshifted MBH
mass

Redshifted BH
mass

Kerr quadrupole
mass moment

Luminosity distance
of the source

The extreme mass-ratio makes the GW emission very inefficient
Evolution in band can last 10^4 – 10^5 orbital cycles
Extremely precise measurements on binary parameters!



Why EMRIs are important?

Quadrupole
mass moment



Test for GR by
spacetime
mapping

Luminosity
distance



Test for
Cosmology

Inclination of
the orbit



Test for the
distribution of COs
around the MBH

Significant
number of EMRIs



Constrain the MBH
mass function

Multimessenger?
No spoiler, see
Zhen talk



How do they form?

High
densities



Dynamical
interactions



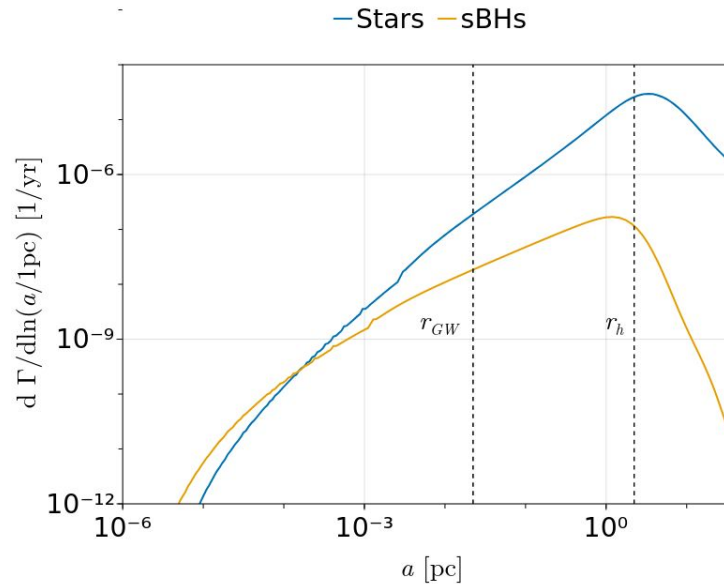
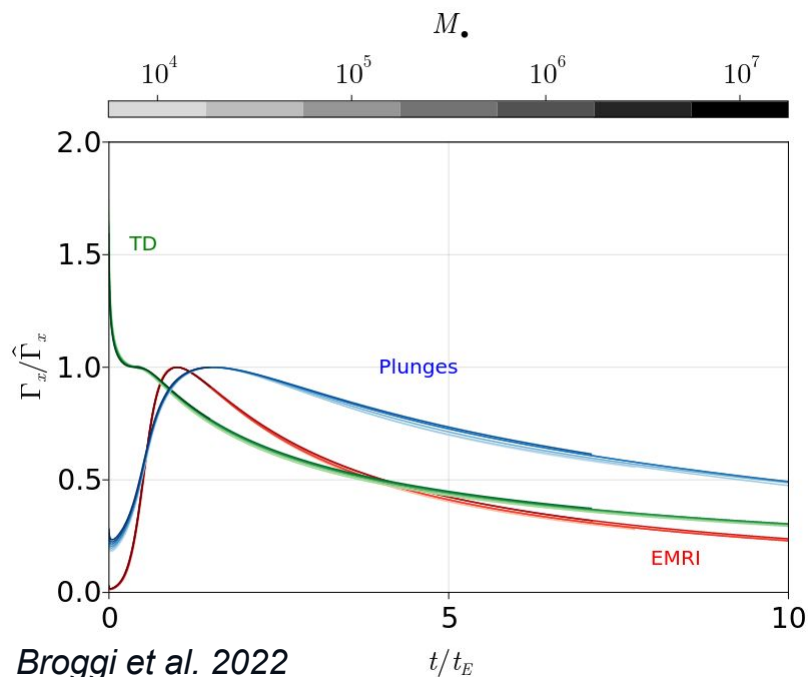
Tidal Disruptions



Direct Plunge



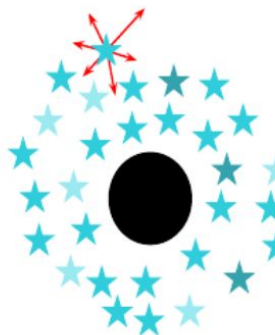
EMRIs



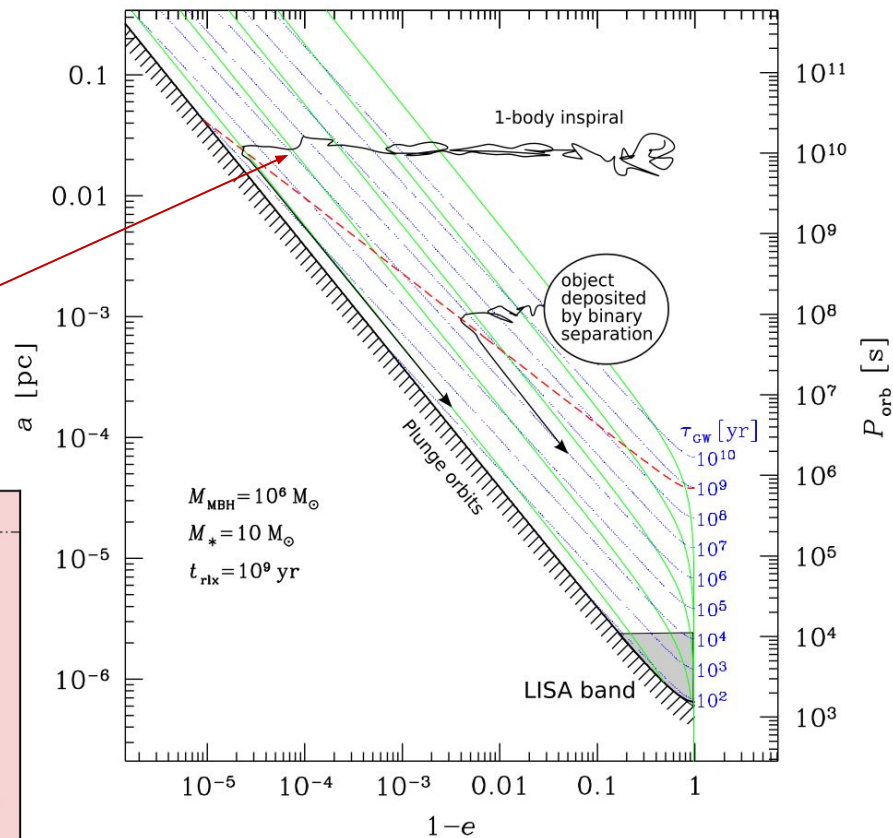
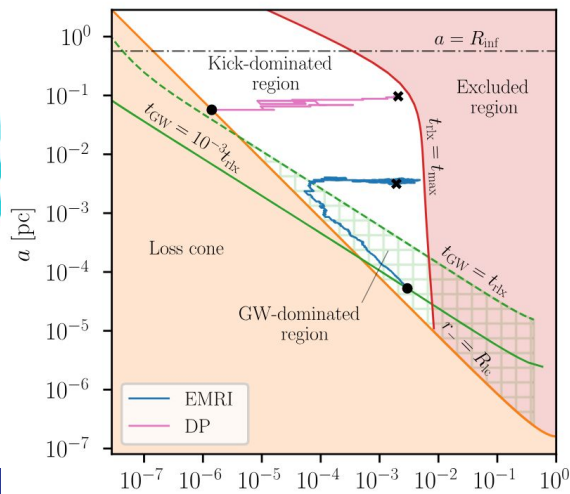
How do they form?

Possible dynamical mechanism...

- Standard Channel: EMRI formation is consequence of two-body relaxation (e.g. Alexander+2017 and many others)



Evolution in angular momentum faster than that in energy



Hopman+2006, Amaro-Seoane+2008, Amaro-Seoane+2012, Vasiliev+2013, Bar-Or+2016, Broggi+2022, Rom+2024, Qunbar+24, Mancieri+2025

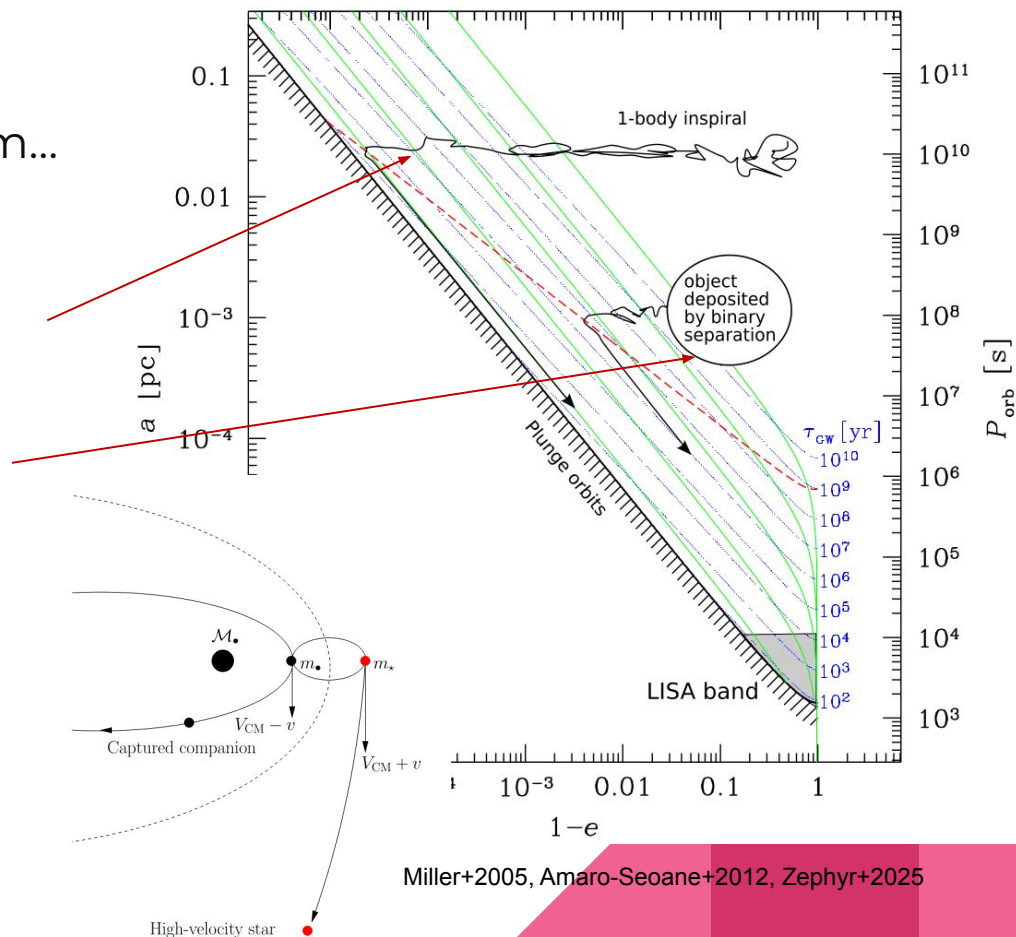
How do they form?

Possible dynamical mechanism...

- Standard Channel: EMRI formation is consequence of two-body relaxation (e.g. Alexander+2017 and many others)
- Binary Tidal Breakup (see e.g. Miller+2005)

$$r_{\text{tide}} \approx (3M/m)^{1/3} a$$

$$\approx 7 \text{ AU} (M/10^6 M_{\odot})^{1/3} (m/10 M_{\odot})^{-1/3} (a/0.1 \text{ AU})$$

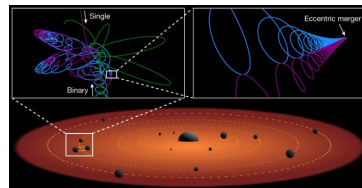
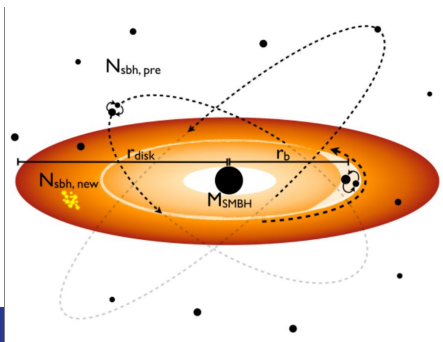


Miller+2005, Amaro-Seoane+2012, Zephyr+2025

How do they form?

Possible dynamical mechanism...

- Standard Channel: EMRI formation is consequence of two-body relaxation (e.g. Alexander+2017 and many others)
- Binary Tidal Breakup (see e.g. Miller+2005)
- BH migration in the disk of AGNs (see e.g. Pan & Yang 2021 + many others)

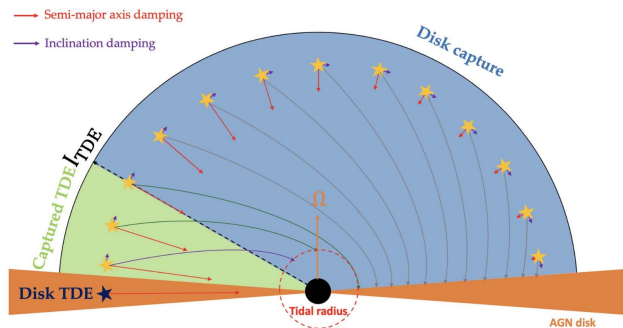


Disk migration/inclination damping

- Type I / Type II migration, depending on mass.
- Drag from gas leads to efficient orbital damping.

Disk-born objects.

- Disk self-gravity may enhance or suppress capture.
- Migration traps, torques, resonances play a role.



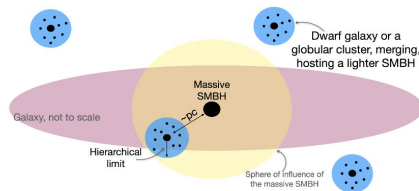
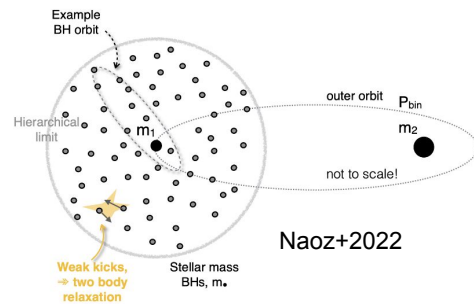
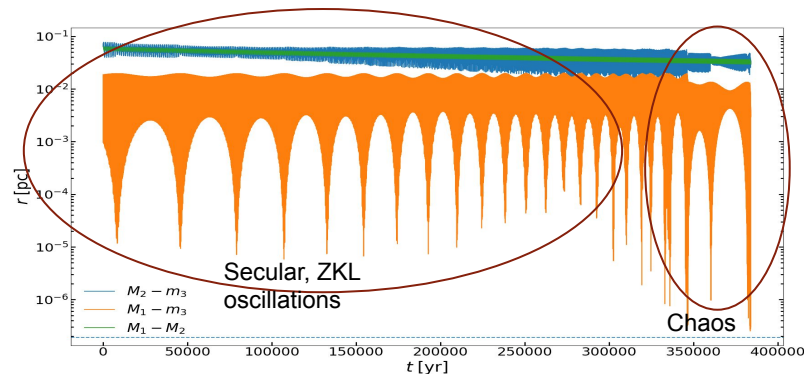
Levin 2007, McKernan+2012/2018, Bartos+2017, Secunda+2019, Tagawa+2020/2023, Wang+2024 Zwick+2024

How do they form?

Possible dynamical mechanism...

- Standard Channel: EMRI formation is consequence of two-body relaxation (e.g. Alexander+2017 and many others)
- Binary Tidal Breakup (see e.g. Miller+2005)
- BH migration in the disk of AGNs (see e.g. Pan & Yang 2021 + many others)
- Perturbation from a second MBH (e.g. Bode+2014, Mazzolari+2022, Naoz+2022 and following)

During the hardening phase of a MBH binary.
Cusp of compact object perturbed by the presence of a bin perturber

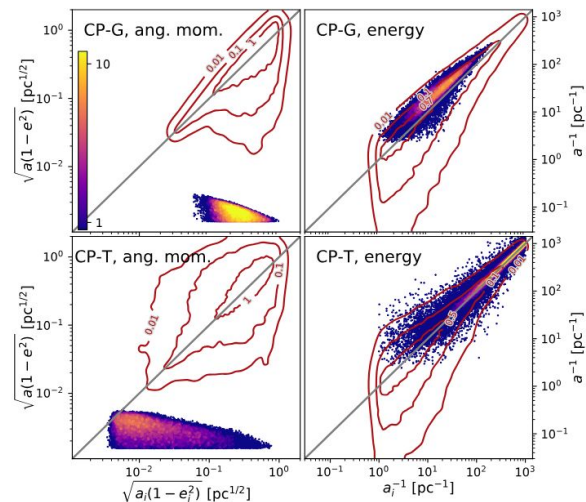


How do they form?

Possible dynamical mechanism...

- Standard Channel: EMRI formation is consequence of two-body relaxation (e.g. Alexander+2017 and many others)
- Binary Tidal Breakup (see e.g. Miller+2005)
- BH migration in the disk of AGNs (see e.g. Pan & Yang 2021 + many others)
- Perturbation from a second MBH (e.g. Mazzolari+2022, Naoz+2022 and following)
- Supernova kicks (Bortolas+2019)

Supernova kicks might send an object close to central MBH, bypassing slow two-body relaxation



Expected features from different scenarios (?)

Channel	Eccentricity	Inclination	Likely nature of secondary
Two-body relaxation	Very high	Uniform*	BHs as they segregate better
Binary tidal separation	Medium	Uniform*	BHs as they segregate better
AGN disk	Almost zero	Almost Aligned	BHs as drag might be efficient
MBH binary	Very high	Uniform/polar**	Depends on objects in the cusp
SN kicks	High	Uniform*	NS generally have higher kicks

*if the MBH is maximally spinning prograde orbits might be favoured (e.g. Amaro-Seoane+2012)

**depends on specific orbital configurations of the triplet

Expected features from different scenarios (?)

Channel	Eccentricity	Inclination	Likely nature of secondary
Two-body relaxation	Very high	Uniform*	BHs as they segregate better
Binary tidal separation	Medium	Uniform*	BHs as they segregate better
AGN disk	Almost zero	Almost Aligned	BHs as drag might be efficient
MBH binary	Very high	Uniform/polar**	Depends on objects in the cusp
SN kicks	High	Uniform*	NS generally have higher kicks

Still, those features are model-specific, no consensus on the quantitative shape of the distributions of parameters

Expected peak rates from different scenarios

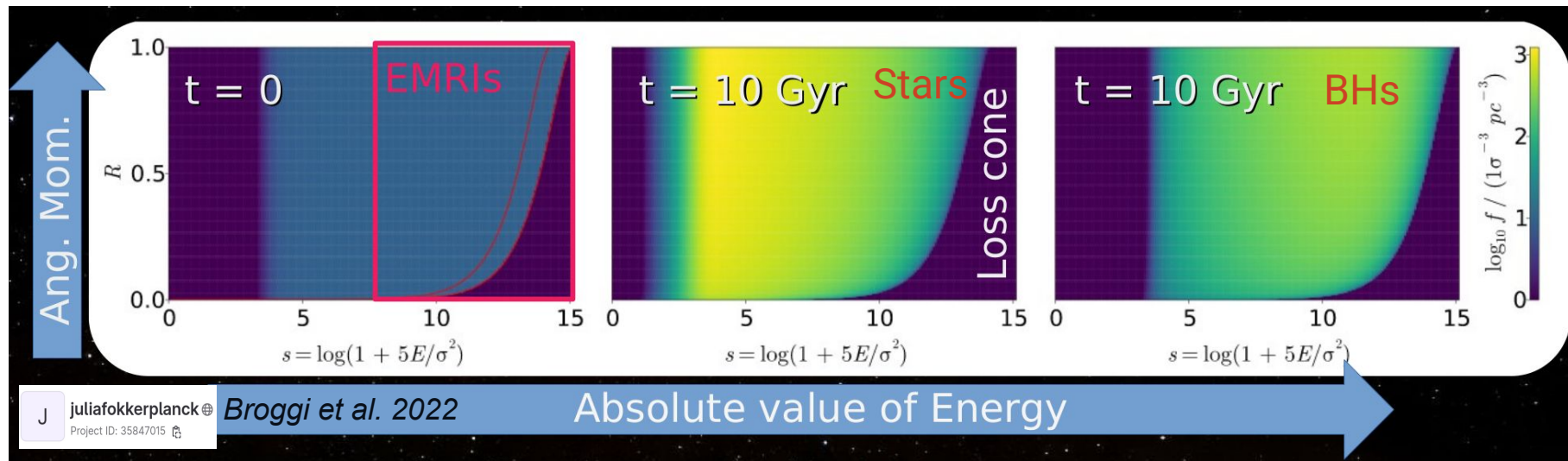
Channel	<u>Peak</u> EMRI rate per galaxy [yr^{-1}]	Main source of uncertainty
Two-body relaxation	few $\times 10^{-8} - 10^{-6}$ (e.g. Broggi+2022)	Shape of nuclear star clusters, stellar mass function
Binary tidal separation	10^{-7} (e.g. Miller+2005)	Shape of nuclear star clusters, unknown primordial binary fraction
AGN disk	$10^{-7} - 10^{-4}$ (e.g. Pan+2021)	Unknown hydro-drag efficiency, semi-analytical based since fully numerical sims are too complex
MBH binary	$10^{-6} - 10^{-5}$ (e.g. Mazzolari+2022)	Shape of nuclear star clusters, MBHB abundance
SN kicks	few $\times 10^{-8}$ (e.g. Bortolas+2019)	Shape of nuclear star clusters, stellar mass function, kick magnitude

Common to all channels: unknown MBH mass function at low masses

Expected rates from different scenarios

Rates are actually **time evolving**, thus the actual number of EMRIs depends on the duration of the process that form them

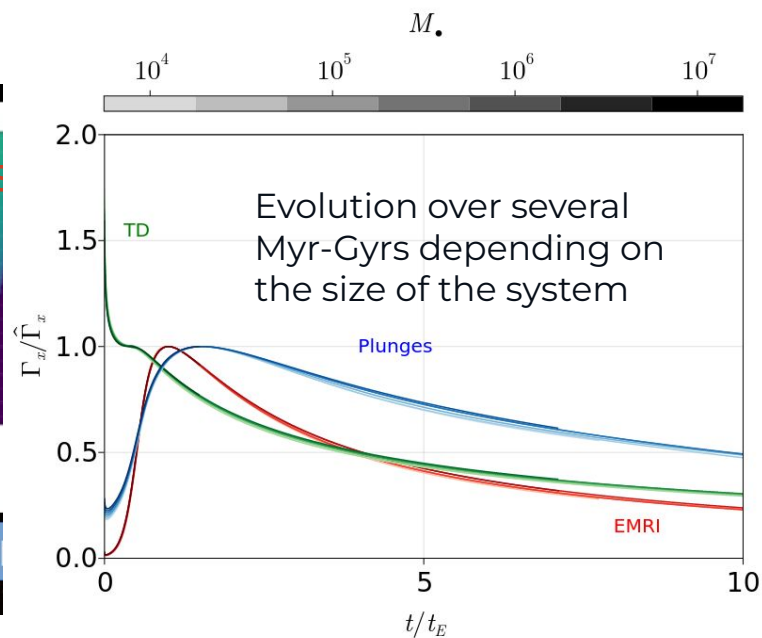
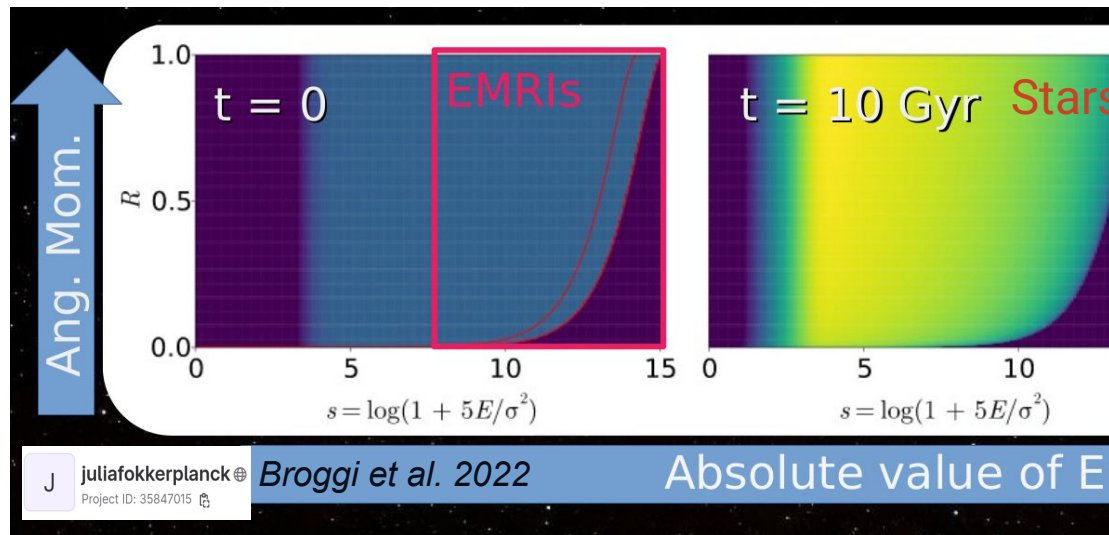
Two-body relaxation: Fokker-Planck approach



Expected rates from different scenarios

Rates are actually **time evolving**, thus the actual number of EMRIs depends on the duration of the process that form them

Two-body relaxation: Fokker-Planck approach



Expected rates from different scenarios

Rates are actually **time evolving**, thus the actual number of EMRIs depends on the duration of the process that form them

AGN disk:

Disk lifetime 1-100 Myr

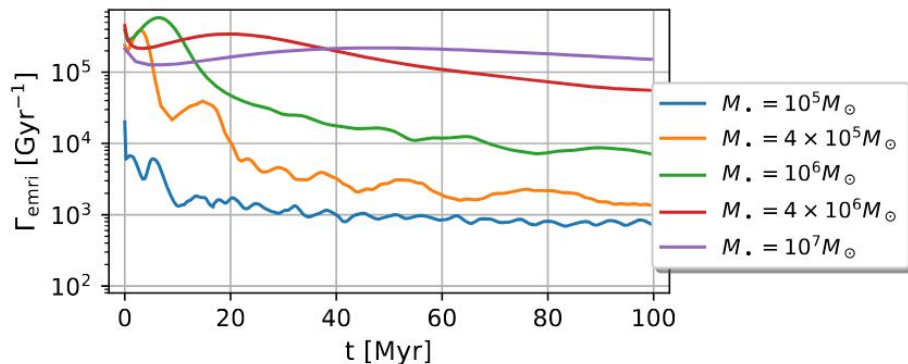
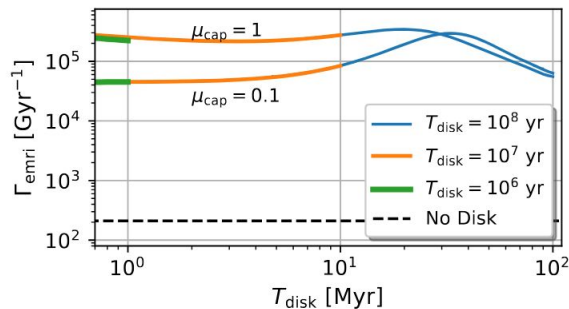


FIG. 11. The disk-assisted EMRI rate $\Gamma_{\text{emri}}(t; T_{\text{disk}} = 10^8 \text{ yrs})$ for different MBH masses M_{\bullet} , where take $\mu_{\text{cap}} = 1$.

Expected rates from different scenarios

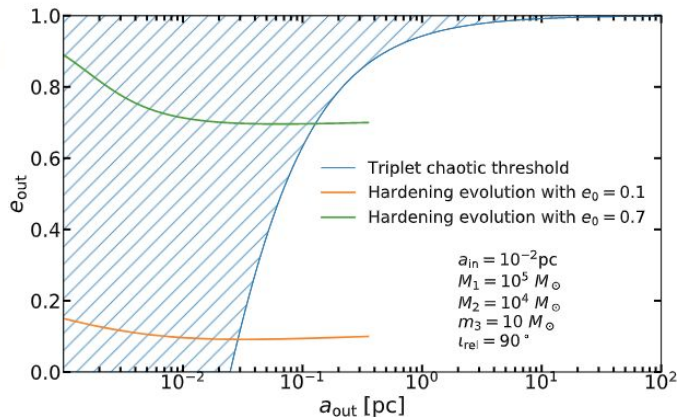
Rates are actually **time evolving**, thus the actual number of EMRIs depends on the duration of the process that form them

MBHB:

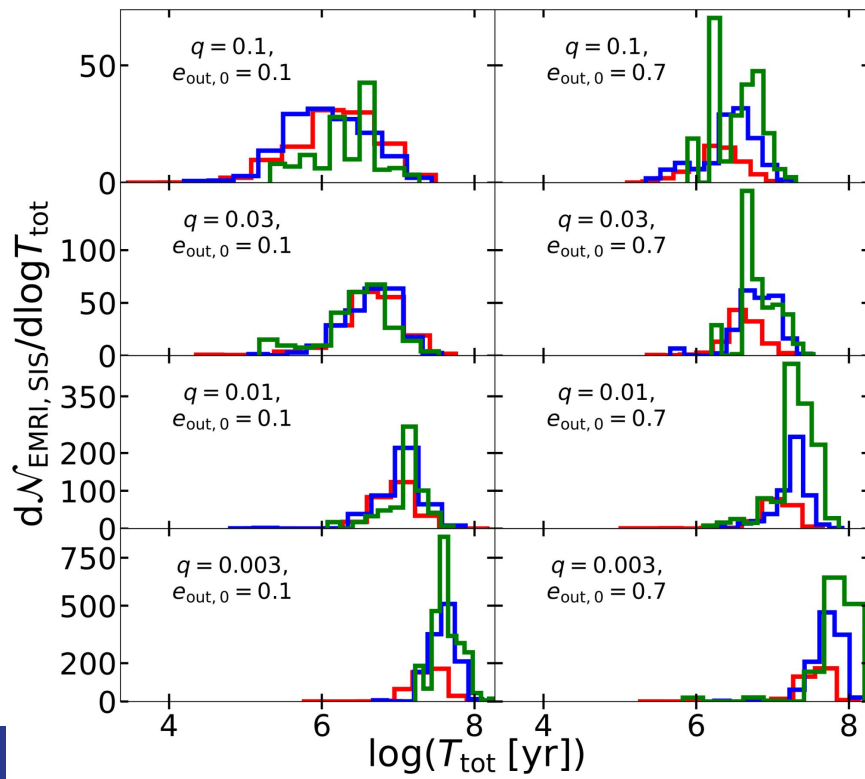
Binary evolves because of stellar hardening on timescales 0.1-1 Gyr

$$\dot{a} = -a^2 \frac{GH\rho}{\sigma}$$

$$\dot{e} = a \frac{GHK\rho}{\sigma}$$



Mazzolari+2022



Expected rates from different scenarios

Rates are actually **time evolving**, thus the actual number of EMRIs depends on the duration of the process that form them

SN kicks:

Requires a young stellar population that undergo supernova explosion, rates enhanced by top-heavy mass function

CWD=clockwise disc

SCL=S star-clusters

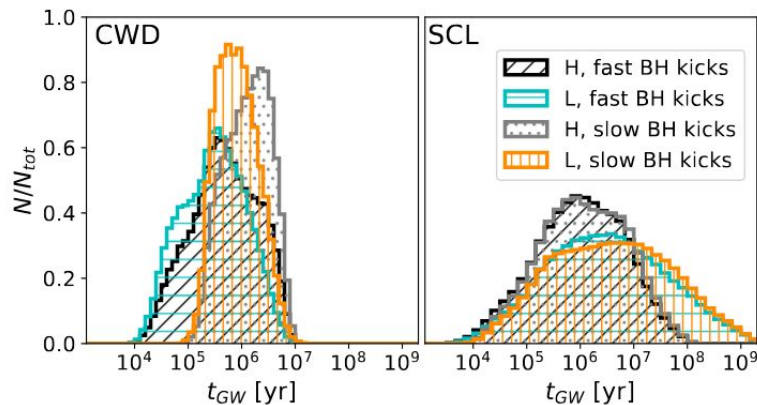


Figure 7. Distribution of the time elapsed from the SN explosion to the final CO coalescence (computed via Eq. 10), for the COs undergoing a SN-EMRI. We show only the CWD (left) and SCL (right) scenarios, as they are representative of the GE and TE cases, respectively. Within each panel, the black and grey (cyan and orange) histograms assume the H (L) background population and the fast and slow BH kick prescriptions, respectively.

An attempt for uncertainty exploration for two-body relaxation

- Semi-analytical relations for EMRI rate
- Coupling with semi-analytical code for MBH evolution in galaxies

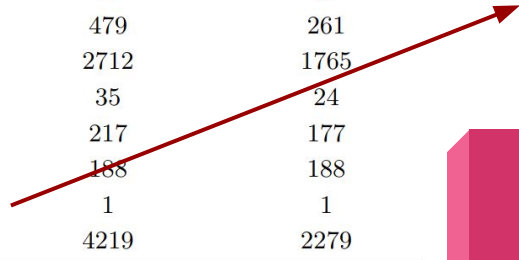
Model	Mass function	MBH spin	Cusp erosion	$M-\sigma$ relation	N_p	CO mass [M_\odot]	Total	EMRI rate [yr^{-1}] Detected (AKK)	Detected (AKS)
M1	Barausse12	a98	yes	Gultekin09	10	10	1600	294	189
M2	Barausse12	a98	yes	KormendyHo13	10	10	1400	220	146
M3	Barausse12	a98	yes	GrahamScott13	10	10	2770	809	440
M4	Barausse12	a98	yes	Gultekin09	10	30	520 (620)	260	221
M5	Gair10	a98	no	Gultekin09	10	10	140	47	15
M6	Barausse12	a98	no	Gultekin09	10	10	2080	479	261
M7	Barausse12	a98	yes	Gultekin09	0	10	15800	2712	1765
M8	Barausse12	a98	yes	Gultekin09	100	10	180	35	24
M9	Barausse12	aflat	yes	Gultekin09	10	10	1530	217	177
M10	Barausse12	a0	yes	Gultekin09	10	10	1520	188	188
M11	Gair10	a0	no	Gultekin09	100	10	13	1	1
M12	Barausse12	a98	no	Gultekin09	0	10	20000	4219	2279

An attempt for uncertainty exploration for two-body relaxation

- Semi-analytical relations for EMRI rate
- Coupling with semi-analytical code for MBH evolution in galaxies

Model	Mass function	MBH spin	Cusp erosion	$M-\sigma$ relation	N_p	CO mass [M_\odot]	Total	EMRI rate [yr^{-1}] Detected (AKK)	Detected (AKS)
M1	Barausse12	a98	yes	Gultekin09	10	10	1600	294	189
M2	Barausse12	a98	yes	KormendyHo13	10	10	1400	220	146
M3	Barausse12	a98	yes	GrahamScott13	10	10	2770	809	440
M4	Barausse12	a98	yes	Gultekin09	10	30	520 (620)	260	221
M5	Gair10	a98	no	Gultekin09	10	10	140	47	15
M6	Barausse12	a98	no	Gultekin09	10	10	2080	479	261
M7	Barausse12	a98	yes	Gultekin09	0	10	15800	2712	1765
M8	Barausse12	a98	yes	Gultekin09	100	10	180	35	24
M9	Barausse12	aflat	yes	Gultekin09	10	10	1530	217	177
M10	Barausse12	a0	yes	Gultekin09	10	10	1520	188	188
M11	Gair10	a0	no	Gultekin09	100	10	13	1	1
M12	Barausse12	a98	no	Gultekin09	0	10	20000	4219	2279

Quite large uncertainty



Possible improvements for two-body relaxation channel

Fokker-Planck approach

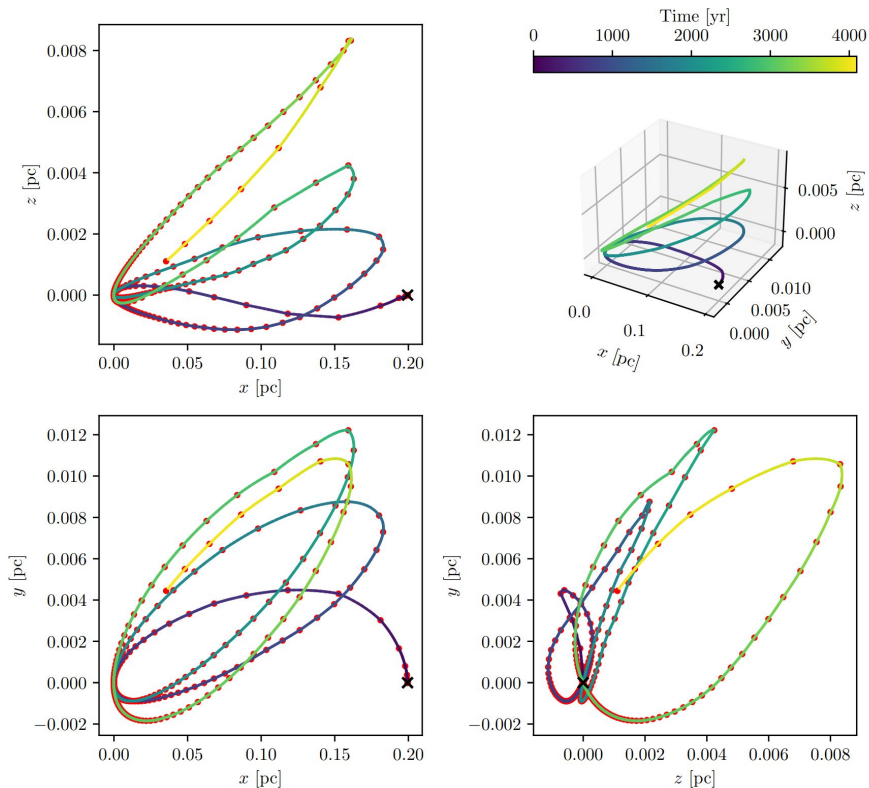
- Relies on mean-field and can evolve multiple stellar populations.
- The inclusion of GWs effects is not straightforward.
- EMRI are found from object below a certain critical semi-major axis, above only plunge

Monte Carlo approach

- Evolve the post-Newtonian (PN) equations of motion of a compact object orbiting an MBH
- Accounts for the effects of two-body relaxation locally on the fly, no orbit-averaging
- Evolves one EMRI systems at a time, so more computational intense

We can combine the two approaches to get more information
See Mancieri+2025 A&A, 694, A272

Possible improvements for two-body relaxation channel



The diffusion coefficients in velocity are then directly related to the parameters of the Gaussian distributions characterising Δv_{\parallel} and a Δv_{\perp} at each time step of the integration:

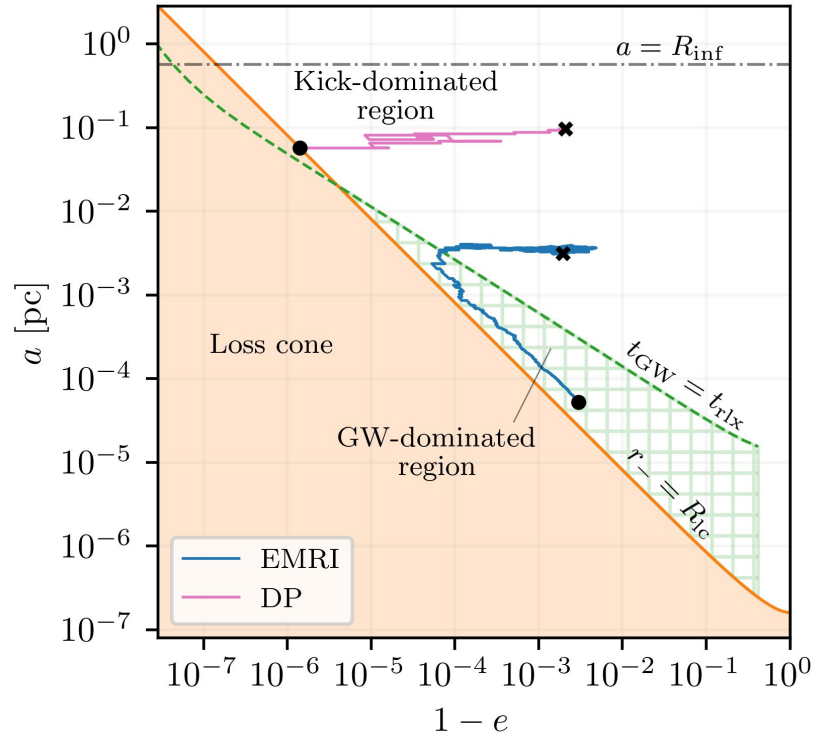
$$\Delta v_{\parallel} = \mu_{\parallel} + s_{\parallel} \sigma_{\parallel}, \quad \Delta v_{\perp} = \mu_{\perp} + s_{\perp} \sigma_{\perp}. \quad (43)$$

Here, s_{\parallel} and s_{\perp} are two uncorrelated random values, each extracted from a Normal distribution, while

$$\begin{aligned} \mu_{\parallel} &= D[\Delta v_{\parallel}] \Delta t, & \sigma_{\parallel}^2 &= D[(\Delta v_{\parallel})^2] \Delta t - (D[\Delta v_{\parallel}] \Delta t)^2, \\ \mu_{\perp} &= 0, & \sigma_{\perp}^2 &= D[(\Delta v_{\perp})^2] \Delta t. \end{aligned} \quad (44)$$

Diffusion coefficients

Possible improvements for two-body relaxation channel

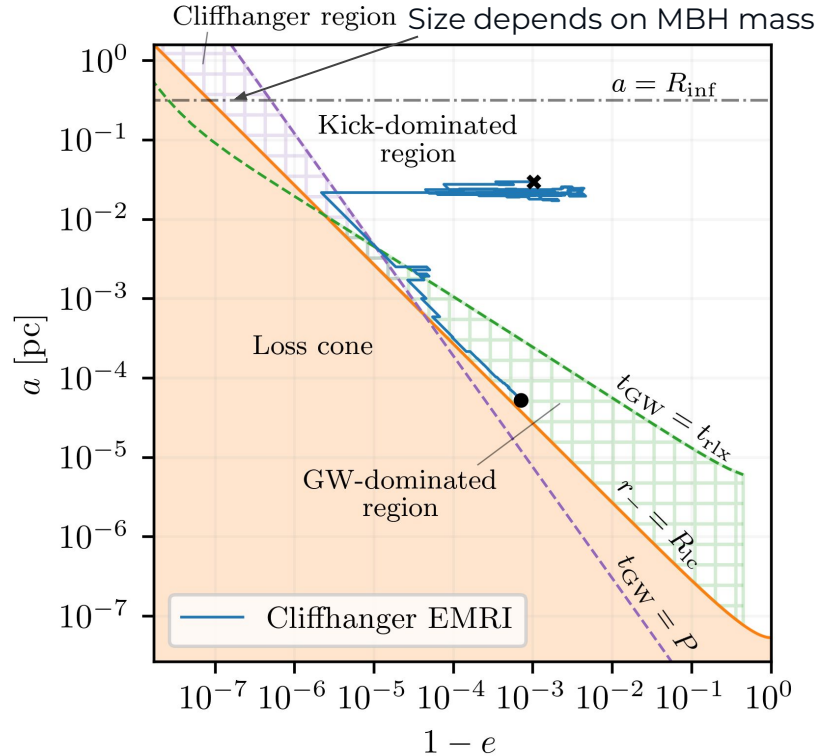


Classical EMRI evolution

Evolution is governed by stochastic kicks, evolution in angular momentum (i.e. eccentricity is much faster).

GW might take over and there an EMRI is formed

Possible improvements for two-body relaxation channel



EMRIs from large separation
Cliffhanger EMRIs (Qunbar+24):

The Monte Carlo approach identifies EMRIs that classically would have been identified as plunges.

Those form when GW emission at pericentre is extremely powerful:

$$T_{\text{gw}} < T_{\text{orb}}$$

We can simulate this given our local approach

Possible improvements for two-body relaxation channel

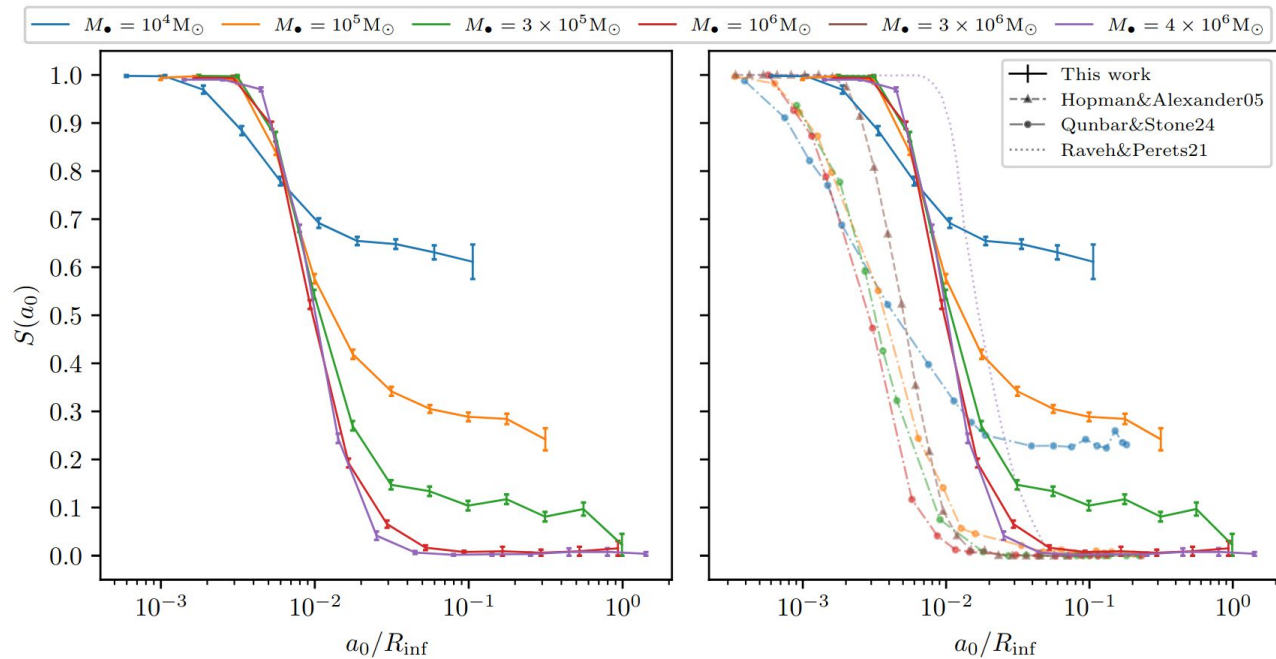


Fig. 9. Function $S(a_0)$ for different M_\bullet scenarios. The bars display 1σ uncertainty. The panel on the left displays our results only, while that on the right compares them with those from other works. We note that the other works make different assumptions, both with respect to our work and to each other.

EMRIs from large separation Cliffhanger EMRIs:

This changes the ratio among EMRIs and plunges

$$S(a_0) = \frac{N_{\text{EMRI}}(a_0)}{N_{\text{EMRI}}(a_0) + N_{\text{DP}}(a_0)},$$

Possible improvements for two-body relaxation channel

Applying the new $S(a)$ transfer function to Fokker-Planck simulations we get that Cliffhanger EMRIs actually represent a large fraction of EMRIs especially around 10^5 Msun

Table 1. Instantaneous EMRI+DP (\dot{N}), EMRI (\dot{N}_{EMRI}), and DP (\dot{N}_{DP}) rates produced in the snapshots we investigated.

M_{\bullet} [M_{\odot}]	t [Myr]	\dot{N} [yr^{-1}]	$\dot{N}_{\text{EMRI}}^{\text{cl}}$ [yr^{-1}]	\dot{N}_{EMRI} [yr^{-1}]	$\dot{N}_{\text{DP}}^{\text{cl}}$ [yr^{-1}]	\dot{N}_{DP} [yr^{-1}]
10^4	0.58	5.9×10^{-7}	5.3×10^{-7}	4.0×10^{-7}	6.5×10^{-8}	1.9×10^{-7}
10^5	11	6.6×10^{-7}	3.1×10^{-7}	2.9×10^{-7}	3.7×10^{-7}	3.8×10^{-7}
3×10^5	25	3.5×10^{-7}	4.9×10^{-8}	6.7×10^{-8}	3.0×10^{-7}	2.8×10^{-7}
3×10^5	45	7.4×10^{-7}	2.0×10^{-7}	2.1×10^{-7}	5.4×10^{-7}	5.3×10^{-7}

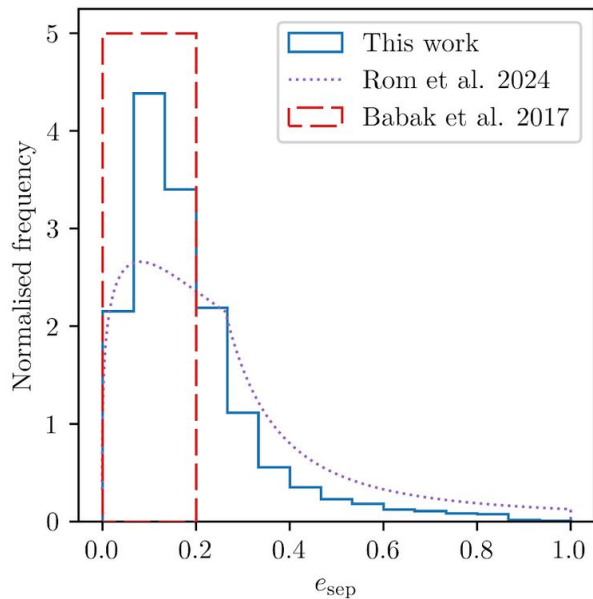
Notes. We report estimates according to our formulation Eq. (62) (no superscript) based on the transfer function $S(a_0)$, and the classical estimates Eq. (64) (superscript cl) based solely on the critical semi-major axis $a_c = 0.01 R_{\text{inf}}$.

This implies that the existence of a class of extremely eccentric EMRIs

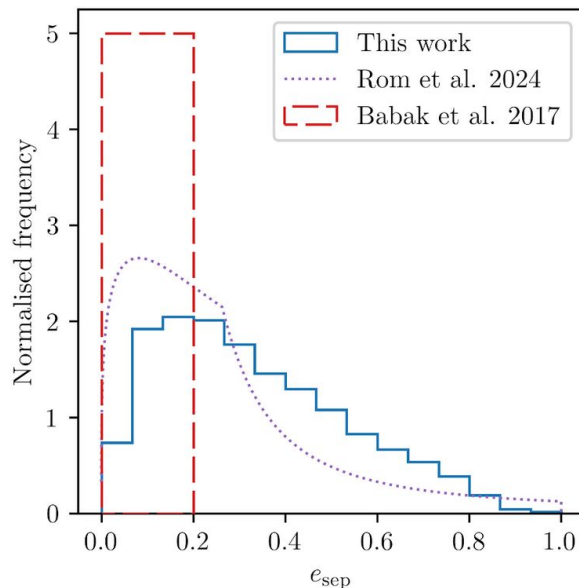
Possible improvements for two-body relaxation channel

This implies that the existence of a class of extremely eccentric EMRIs (IC taken from PN simulations, evolved with FEW v2 until separatrix)

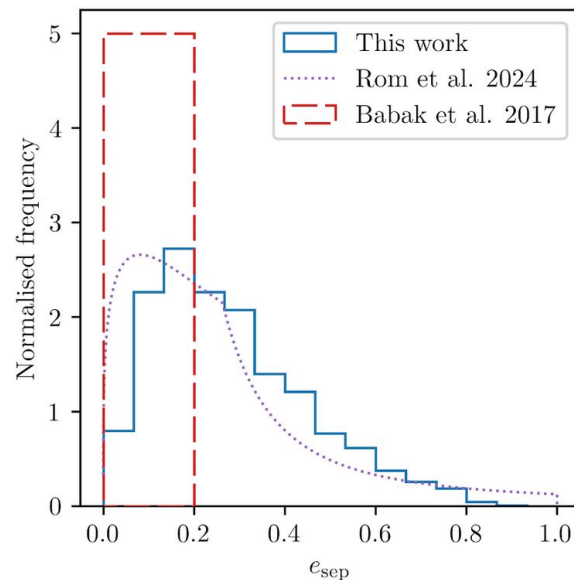
10^4 Msun



10^5 Msun



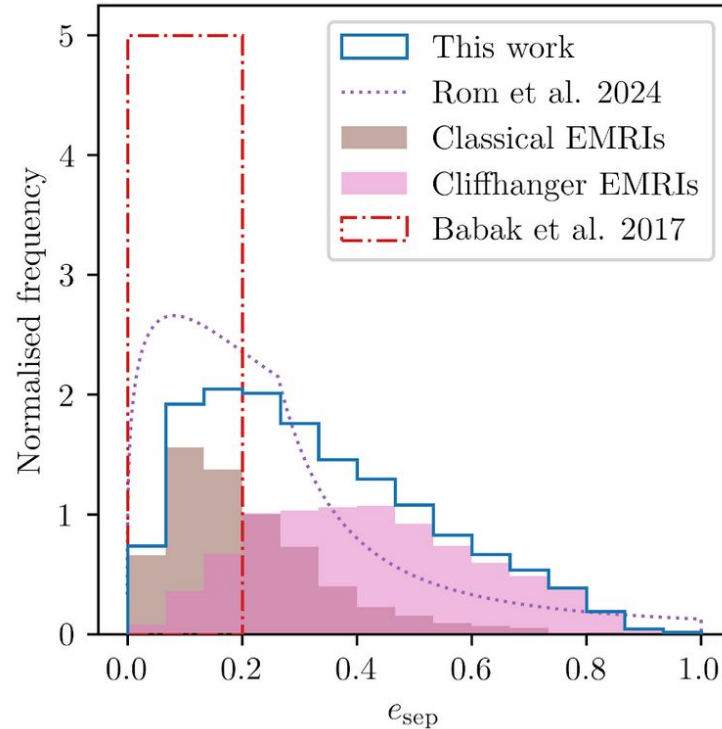
10^6 Msun



Possible improvements for two-body relaxation channel

This implies that the existence of a class of extremely eccentric EMRIs (IC taken from PN simulations, evolved with FEW v2 until separatrix)

10^5 Msun



Further developments and long/mid term plan

Accurate dynamics (Davide Mancieri)

PN expansion might not be super good below $\sim 15R_g$.

We plan to investigate the formation of EMRIs using Kerr geodesic + stochastics kick + radiation reaction

Galactic nucleus modelling (Luca Broggi)

Use of 2-D Fokker-Planck code to evolve multiple stellar components. Find EMRI using input from accurate simulations

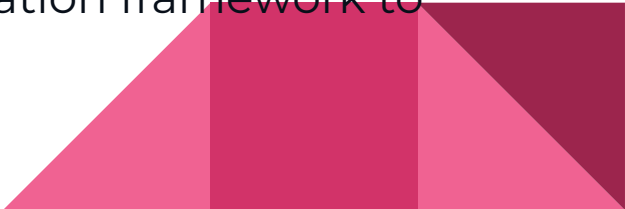
Cosmic evolution (David Izquierdo-Villalba, Polkas+24)

Couple the galactic nucleus evolution with L-galaxies, a semi-analytical code for galaxy-MBH evolution



Most astrophysically accurate EMRI population to date

Conclusions

- EMRI formation is a complex phenomenon, multiple formation channels exists and have been explored in different depth
 - Astrophysical uncertainties remain high, both in rates and EMRI properties
 - Advancements for two-body relaxation channel are ongoing, we could envisage systematic approaches also for other formation channels
 - Final goal is to produce LISA-interpretable results to help data analysis development.
After detection the tools will serve as an interpretation framework to extract astrophysical information from LISA data.
- 

MBHs and host
profiles
at L-Galaxies substep

+ PhaseFlow multi-dimensional grids

→ TDE rates
per galaxy
at L-Galaxies substep

